5136 *Chem. Mater.* **2009,** *21,* 5136–5144
DOI:10.1021/cm9018953

CHEMISTRY OF MATERIALS
Article

Metal Nitride and Metal Carbide Nanoparticles by a Soft Urea Pathway

Cristina Giordano,* Christian Erpen, Weitang Yao, Bettina Milke, and Markus Antonietti

Max-Planck-Institute of Colloids and Interfaces, Colloid Chemistry Research Campus Golm, Am Muehlenberg, D-14476 Golm, Germany

Received June 30, 2009. Revised Manuscript Received September 17, 2009

An easy way to produce several metal nitrides and metal carbides at relatively low temperature (800 °C) using simple and mainly nontoxic precursor is presented. The procedure has been shown to be rather general and it was possible to synthesize TiN, VN, NbN, GaN, Mo_2N, W_2N, CrN, NbC(N), TiC(N), WC, Mo_2C, and Cr_3C_2 nanoparticles using urea or close derivatives as both nitrogen or carbon source and the growth controlling system. In every case, a homogeneous gel-like starting product has been formed that is converted by calcination into the corresponding metal nitride or metal carbide (including mixed species), without any preliminary treatments or further purifications. Samples were characterized by XRD, TEM, SEM, EA, and BET, and the products were shown to be well-defined and rather homogeneous.

Introduction

Finding a general procedure to produce a whole class of materials in a similar way is a desired goal of material chemistry. In our times, this is especially true for nanostructures, as their most charming feature, i.e., possessing novel properties, often means facing unpredictable behavior. This is why still many relevant materials were never made as well-defined nanostructures, or their nanosynthesis is just very incompletely covered. If such a procedure is also simple, cheap, relatively green and safe, it shows the promise for broader application and scalability. In this paper, we present an easy way to produce metal nitride and carbide nanostructures in a pretty general way. As a nontoxic nitrogen/carbon source, urea, guanidine, and some derivatives of these compounds were selected, which simultaneously play the role of an intermediary solvent and stabilizing agent in the early phases of the particle formation reaction.

Despite the considerable presence in literature of papers about synthesis of MN, MC and their ternary compounds (such as MO_xN_y, MO_xC_y, and MC_xN_y), a general safe and competitive synthetic procedure to simplify and scale up their production as nanostructures is still looked for. The high current interest toward MN, MC_xN_y, and MC is mostly due to the wide range of potential applications. Every early transition metal nitride exhibits high chemical stability and functional physical properties such as hardness, high wear resistance, electrical conductivity, or even superconductivity. For example, TiN is used particularly as coating agent for cutting tools, but also as catalyst; GaN finds application in semiconductor devices for optoelectronics,[1] whereas VN is a hard refractory material with metallic properties and used for electrodes in supercapacitors.[2] NbC, TaC, WC, and Mo_2C are powerful catalysts, and especially the two latter are considered potential substitutes of noble metal in catalysis.[3]

Procedures that allow the production of more than one MN or MC are already known in literature, but either they use potentially harmful compounds such as cyanamide at higher temperatures (> 1000 °C),[4] or when using urea, longer and more complicated pathways are requested. In particular, crystalline metal-urea complexes have been used as precursors, presumably because of the ability to isolate and purify them by crystallization.[5,6] In previous experiments, urea has been used exclusively as nitrogen source to address the synthesis of metal nitrides,[7,8] although its usefulness in making metal carbides was shown just recently.[9] In this paper, it was also delineated that working with the clear and homogeneous polymeric or gel-like metal-urea precursor rather than crystalline species allows addressing a much broader range of samples by simple variation of the metal-urea ratio. Especially particle size and the carbon/nitrogen content within the nanoparticle can be varied that way.[9] With this paper, we like to show that the procedure can be applied to a wide range of metals to generate well-defined and highly crystalline nanoparticles of the corresponding carbides and nitrides. By changing from urea to guanidine and other related compounds, we will also analyze how

*Corresponding author.

(1) Ambacher, O. *J. Phys. D: Appl. Phys.* **1998**, *31*(20), 2653.
(2) Choi, D.; Blomgren, G. E.; Kumta, P. N. *Adv. Mater.* **2006**, *18*(9), 1178.
(3) Levy, R. B.; Boudart, M. *Science* **1973**, *181*(4099), 547.
(4) Li, P. G.; Lei, M.; Tang, W. H. *Mater. Res. Bull.* **2008**, *43*(12), 3621.
(5) Gomathi, A.; Sundaresan, A.; Rao, C. N. R. *J. Solid State Chem.* **2007**, *180*, 291.
(6) Sardar, K.; Dan, M.; Schwenzer, B.; Rao, C. N. R. *J. Mater. Chem.* **2005**, *15*(22), 2175.
(7) Qiu, Y.; Gao, L. *Chem. Lett.* **2003**, *32*(8), 774.
(8) Qiu, Y.; Gao, L. *J. Am. Ceram. Soc.* **2004**, *87*(3), 352.
(9) Giordano, C.; Erpen, C.; Yao, W. T.; Antoniett, M. *Nano Lett.* **2008**, *8*(12), 4659.

Published on Web 10/07/2009

Table 1. Experimental details of Some Representative Metal Nitride Products Obtained by Heating Treatment at 800 °C

metal precursors	R[1]	N (wt %)	C (wt %)	expected product	surface area (m^2/g)	nominal diameter (nm)	
						by XRD	by TEM
$MoCl_5$	1	7.2	0.07	Mo_2N	12	19.6	20−40
WCl_4	1	3.58	0.16	W_2N	64	2.6	2−10
$NbCl_5$	3	11.4	0.4	NbN(O)	23	15	10−20
$CrCl_3 \cdot 6H_2O$	3	5.9	4.9	CrN	95	28	15−25
$TiCl_4$	4	15	3.2	TiN	~ 200	10	10−20
$GaCl_3$	0.5	9.9	10.5	GaN	n.m.	5	5−8
$VOCl_3$	3	13.3	14.5	VN	300	11	5−15

[1] R = urea/metal precursors molar ratio. It is considered here to be the minimum value needed to obtain a single-crystalline phase.

variation of the nitrogen source enters the chemical reaction and what additional features can be brought in by this orthogonal synthesis parameter.

Experimental Section

To test the versatility of this pathway, we applied a range of diverse metal salts. In every case, the procedure is the same: appropriate amounts of ethanol (usually 2 g) were mixed with an opportune amount of the selected metal precursor (usually 1 g); for titanium and vanadium samples, the corresponding metal chloride (liquid) was added to ethanol; in all other cases, ethanol was added to the metal chloride powder to reach the targeted concentration (experimental details are reported in Table 1). The metal precursor reacts−partly vigorously−with the alcohol, releasing major parts of the chlorine as HCl and forming the corresponding metal-orthoesters. Chromium samples make an exception as HCl is not released in this step. In every case, a clear solution was obtained. The major restriction of the technique lies in this simple first step: metal salts that do not dissolve and/or react in ethanol cannot be further processed. This restriction, however, can usually be bypassed by a variation of the metal source, e.g., chromium chloride does not dissolve in ethanol, whereas chromium chloride hydrate does. Then, a varying amount of solid urea or related nitrogen source was added slowly to the alcoholic solution to give the specific urea/metal precursor molar ratio (R). This dispersion was stirred until the urea was completely solubilized and the solution was completely clear. Dissolution time depends on the ratio but usually is less than 2 h.

Vanadium prepared with higher ratio ($R > 8$) represents an exception. Indeed, despite a clear dark-reddish solution is obtained within an hour, we preferred to wait one night before the heating treatment. This is in order to complete the bonding with urea and having the vanadium in a final oxidation state of 4+. In terms of colors, this means to wait until the gel turns from reddish to blue, going over a green intermediate color. For $R \leq 3$, a change in color was never observed, even when waiting several days.

It also worth noting that in the presence of the metal precursors, the solubility of urea (or similar compounds) is significantly higher than in pure ethanol (4.877 g/100 g at 18.2 °C), which already indicates the formation of soluble complexes and coordination polymers. In accordance with the FT-IR results (see Figure SI1 and Table SI1 in the Supporting Information), the metal ethoxide is linked with urea through its carbonyl group and can even replace the ethoxide group bonded to the metal, when the urea/metal molar ratio increases. This is backed by a whole set of systematic variations. The intensity of the carbonyl group stretching vibration decreases until it disappears with increasing urea/metal molar ratio, whereas the C−N stretching vibration shifts to higher wavenumber with respect to the pure urea, indicating a stronger bond between C and N. Changes both in peaks positions and intensities of the $-NH_2$ group bending and stretching vibrations indicate an intermolecular linkage between urea molecules.

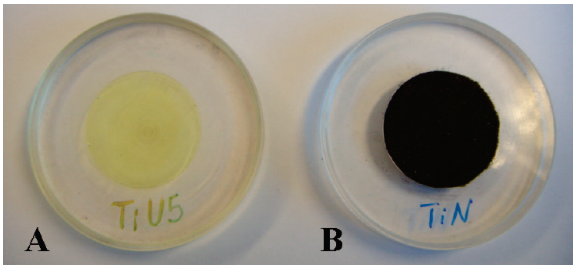

Figure 1. Titanium-urea gel at $R = 5$ (A) before and (B) after heating treatment at 800 °C. It can be nicely seen that before temperature treatment the nitride precursor can be dried into a glassy film, whereas after temperature treatment a finely dispersed powder is obtained.

In line with this observation, different metal salts can solubilize different maximal amounts of urea, reflecting the different coordination sphere and gel structure. This is why the maximal ratio between urea and metal salt (R) is restricted in some cases. In case of titanium, for example, the maximum molar ratio achieved is $R = 14$, whereas for tungsten and molybdenum it is $R = 7$ and for gallium only $R = 1.5$. The result on gallium was particularly surprising, considering that within a similar procedure a urea/metal molar ratio of 6 was reported for the crystalline complex.[7]

Using an ultrasonic bath or heating is not necessary to obtain homogeneity, but in some cases we used it to speed up the process, without observing any changes in the gel texture. These viscous solutions can be dried into a glass or glassy film (Figure 1A), thus enabling al processes like spray coating, spinning, printing, or templating.

The gels were then put into an oven and treated under a N_2 flow at 800 °C for 3 h (plus 4 h to reach the final temperature). Here it is important to underline that the heating treatment is the only sensitive step of the whole procedure. It is necessary to increase the temperature slowly (~3 °C per min) to avoid excessive foaming of the polymer-like cohesive gel and eruptive release of the leftovers of the solvent. It is also then mandatory let the products cool down before exposing them to air; otherwise, for some more reactive systems, partly explosive oxidation of the nanoparticles and/or the presence of unwanted side-products such as metal oxides can occur. After the correct heat treatment, the samples can, however, be stored for several months without any special equipment; they are especially stable against oxidative atmosphere. In all cases, a dark finely dispersed powder has been obtained, with bronze or greenish reflections in case of TiN (Figure 1B) and CrN, respectively, and silvery-black for all other metals.

Vanadium again represents an exception, forming solid silvery-gray foams, which is presumably related to a high

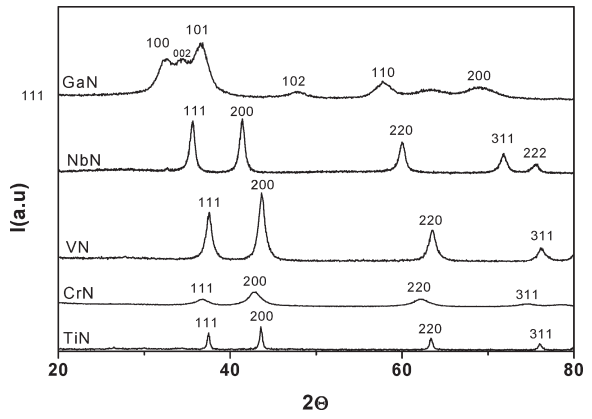

Figure 2. Exemplary XRD pattern for TiN, CrN, VN, NbN, and GaN samples.

cross-linking density and mechanical stability of the secondary metal-urea precursor gel. This finding implies the necessity to heat up vanadium gels in crucibles filled less than a quarter.

Finally, it is worth noting that no further purification is necessary before or after the temperature treatment, especially no solid precipitations, recrystallization, and no side reactions or major side products are observed when keeping the process. Particularly, the amount of amorphous carbon, a typical side product of MN formation, can be kept very low (see also table 1). Species identification was performed according to elemental analysis and X-rays diffraction (by ICDD-PDF4+ database). XRD measurements were performed on a D8 Diffractometer from Bruker instruments (Cu Kα radiation, $\lambda = 0.154$ nm) equipped with a scintillation counter. Nitrogen sorption experiments were done with a Quantachrome Autosorb-1 or Quadrasorb at liquid nitrogen temperature, and data analysis were performed by Quantachrome software. All the samples were degassed at 150 °C for 20 h before measurements. Elemental analysis was done for Carbon, Hydrogen, Nitrogen using a Vario EL Elementar. TEM images were taken using a Zeiss EM 912Ω operated at an acceleration voltage of 120 kV. Samples were ground and then suspended in ethanol. One drop of this suspension was put on a 400 mesh carbon-coated copper grid and left to air to dry. A HRTEM Philips CM 200 LaB6, operated at an acceleration voltage of 200 kV was also used. SEM was performed on a LEO 1550 Gemini instrument. The samples were loaded on carbon coated stubs and coated by sputtering an Au/Pd alloy prior to imaging. TGA measurements were performed under nitrogen between 50 and 1000 °C (heating rate 10 K/min) with a TG 209 F1 Iris, Netzsch.

Results and Discussion

Using urea, single phase metal nitrides can be obtained keeping the urea/metal precursors molar ratio (R) lower than 4 (Table 1).

The absence of side crystalline products as well as high crystallinity of the sample can be deduced from Figure 2, where the XRD patterns of some MN are shown. X-ray sizes, estimated by the Scherrer's equation from the (200) peak of the cubic structures of TiN, VN, NbN, and CrN, are in any case less than 30 nm diameter, and they are in good agreement with the size obtained by TEM investigation (table 1). For the gallium sample, because of the broadening of the main diffraction peaks characteristic for nanoparticles, sizes have been estimated from the isolated (102) peak of the hexagonal structure of GaN. It will be shown below (Figure 4) that increasing the ratio R leads to sharper peaks, indicating larger crystalline structures ($d \approx 50-100$ nm). Results about molybdenum and tungsten samples have been previously reported and therefore will be not repeated here.[9]

In the case of niobium, the sample with $R = 1$ showed an XRD pattern constituted by a complex mixtures of niobium oxides (mainly NbO_2 and Nb_2O_5) and oxy-nitride, whereas for $R = 3$, a single-crystalline phase and no further (crystalline) byproduct was found. However, the peak positions of the $R = 3$ sample are shifted to higher angles as compared to the expected NbN pattern, and the experimental patterns are rather closer to a nonstoichiometric oxy-nitrides (tentatively attributed to $Nb_{3.49}N_{4.56}O_{0.44}$, ref ICDD-PDF4+ 04−011−6182) indicating that still some oxygen atoms have been kept in the structure of the NbN. Increasing the ratio to $R = 5$ finally reveals the pure nitride (the experimental pattern of Nb-urea derived sample at $R = 5$ is reported in Figure 2), and the reflexions can be indexed to the cubic phase of NbN (ref ICDD-PDF4+ 04−008−5125). The size of the nanoparticles within these composition variations stays at around $d \approx 15$ nm.

The very oxophillic titanium is similar to the niobium case, but shifted to even higher ammonia surplus. For $R = 3$, both TiN and TiO_2 peaks can be seen (Figure 4A). The fact that for titanium sample at $R = 3$ the XRD peaks are shifted by about 0.5° with respect to the expected positions for pure TiN, while TiO_2 peak positions are almost unaffected could indicate the formation of an oxy-nitride, but an unambiguous attribution is not possible on the basis of X-ray data only. Further experiments are currently in progress in order to ascertain this interpretation. The importance of metal oxy-nitride compounds (particularly titanium oxy-nitride) is mainly due to their application in photocatalysis.[10,11] Pure TiN is obtained only for $R > 3$, again a sign to the high oxophilicity of Ti.

Table 1 also shows that, with a few exceptions, the amount of residual carbon is lower than 0.5%. But even the 3% carbon for TiN is already quite acceptable, considering that the carbon amounts usually reported are higher.[12]

X-ray data were then confirmed with TEM and HR-TEM experiments. Samples for TEM were prepared dispersing a small amount of solid powder in ethanol and using in some cases an ultrasonic bath to help powder dispersion, in every case without addition of any further dispersing agent. Some typical TEM pictures are shown in Figure 3.

For TiN and NbN, spherically shaped, well-defined nanoparticles, just weakly interacting, can be seen (note that any stabilizer is absent). Figure 3C shows a special

(10) Hitoki, G.; Takata, T.; Kondo, J. N.; Hara, M.; Kobayashi, H.; Domen, K. *Electrochemistry* **2002**, *70*(6), 463.
(11) Martinez-Ferrero, E.; Sakatani, Y.; Boissiere, C.; Grosso, D.; Fuertes, A.; Fraxedas, J.; Sanchez, C. *Adv. Funct. Mater.* **2007**, *17*, 3348.
(12) Fischer, A.; Antonietti, M.; Thomas, A. *Adv. Mater.* **2007**, *19*(2), 264.

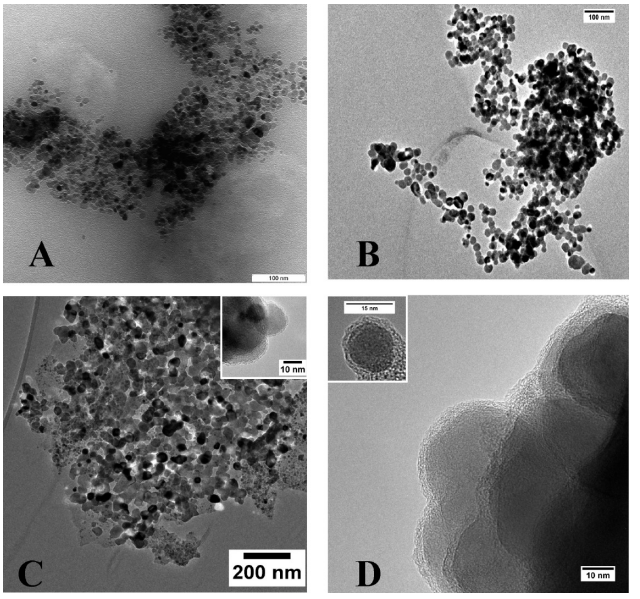

Figure 3. TEM images of (A) TiN (scale bar 100 nm), (B) NbN (scale bar 100 nm), (C) VN, and (D) CrN (inset scale bar 15 nm) nanoparticles.

picture of VN nanocrystals, here still in coexistence with some primary amorphous nanoparticles, from which they obviously form from.

Interesting for VN and CrN cases is that the residual carbon is not an ill-posed side product, but it is found as an extremely defined, ca. 2−4 nm thick coating around the particles. HRTEM images of VN and CrN nanoparticles are shown in the insets of C and D in Figure 3, respectively. For both VN and CrN, the well-defined, single-crystalline character of the particles is reflected in the presence of a continuous grid of reticular planes inside the particle. For CrN, the interplanar distance calculated from the picture is 2.072 Å, corresponding to the d_{200} plane of CrN bulk. This is in good agreement with the expected value (d = 2.0745 Å) for cubic CrN (ref ICDD-PDF4+ 04−008−7177). One can also see the high homogeneity and inner structure of the carbon coating, which is typical for defect-rich, graphitic carbon. For VN the interplanar distance calculated from TEM images on its nanocrystals is 2.38 Å corresponding to the d_{111} plane of VN bulk, also in good agreement with the expected value (d = 2.3896 Å) for cubic VN (ref ICDD-PDF4+ 00−035−0768). We interpret this finding by the enrichment and final release of carbon from the amorphous intermediate particle by the growing crystal front. Crystal structures that obviously do not tolerate major substitution of nitride positions by carbon then can form such a nanocomposite, the size of which is defined by the primary amorphous nanoparticle and the formation of the growth inhibiting carbon layer. The quite perfect refining of the lattice distance indeed support the view that in case of VN and CrN, rather pure nitrides are formed.

From Figure 3C, a mesoporous character of the larger, tectonic VN mesocrystals can be observed, which is confirmed from the very high surface area exhibited by the vanadium samples (Tables 1 and 2).

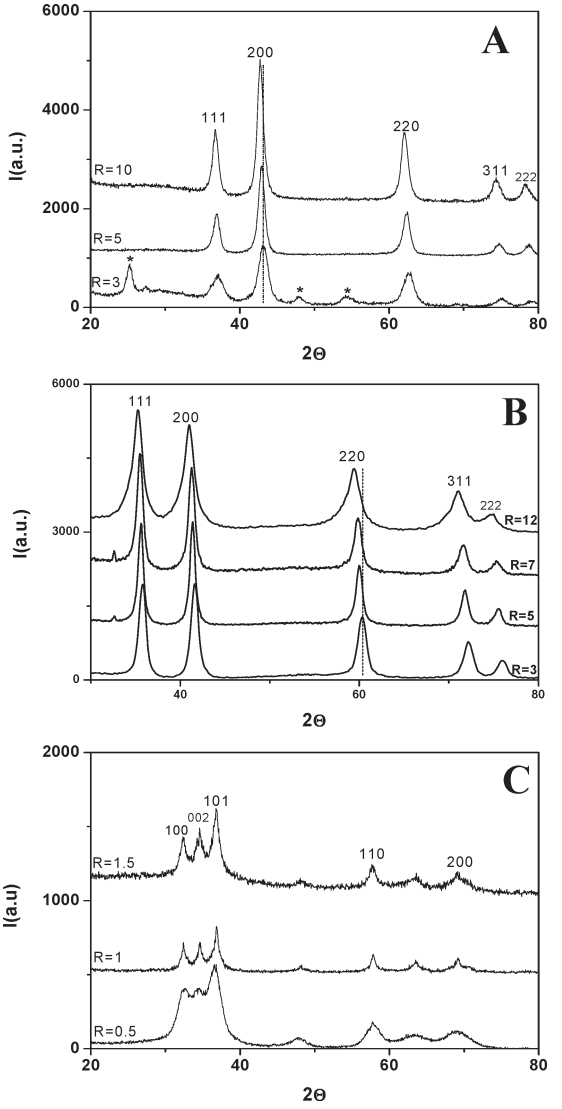

Figure 4. XRD pattern of (A) titanium, (B) niobium, and (C) gallium-urea derived samples at different urea/metal precursor molar ratios (R). In A, marked peaks are attributed to TiO_2.

Another interesting behavior of the (metallic) VN is found in many of the pictures, but also in XRD. Well-defined species show a tendency to a cooperative behavior which could be easily tuned to switch from individual and isolated particles to more organized network structures, and vice versa, simply by adjusting the synthetic procedure (e.g., reaction time). Such "crystals of crystals" or mesocrystals were already observed in previous studies, for instance for SnO_2 nanoparticles[13,14]

Further investigation of this effect and those particles is rather extensive and has to be addressed in an independent paper.

Finally, the finding of the direct synthesis of VN@C and CrN@C nanocomposite particles is very interesting as the carbon shell can add peculiar properties to the nanoparticles, e.g., improving catalytic potential in the

(13) Ba, J.; Feldhoff, A.; Fattakhova-Rohlfing, D.; Wark, M.; Antonietti, M.; Niederberger, M. *Small* **2007**, *3*(2), 310.
(14) Antonietti, M.; Niederberger, M.; Smarsly, B. *Dalton Transactions* **2008**, No. 1, 18.

Table 2. Experimental Details on Samples Obtained at Higher *R*

metal precursors	urea/metal precursors molar ratio	N (wt %)	C (wt %)	expected final product	surface area (m^2/g)	nominal diameter (nm) by XRD	nominal diameter (nm) By TEM
$GaCl_3$	1.5	19.3	19.4	GaN[a]	25	11	3−10*
$TiCl_4$	10	14	21	TiC(N)	200	10	10−20
$NbCl_5$	10	5.4	7.3	NbC(N)	140	8	10−15
$VOCl_3$	8	10.6	26.0	VC(N)[b]	450	20	10−30
$MoCl_5$	7	1.28	5.26	Mo_2C	22	21	15−30
WCl_4	7	1.69	4.90	WC	84	4	3−6

[a] GaN nanoparticles have been observed together with larger crystals with an average size of 50−100 nm (as reported in the text). [b] From the XRD pattern, we cannot differentiate if is VC(N) or VN(C).

case of CrN or potentially better performances as supercapacitor in case of VN. Also, a higher chemical resistance and longer durability is expected. In any case, it allows the chemical addressability of such particles by the known set of carbon functionalization reactions, e.g., for a better dispersibility in a variety of solvents or for applications as a coating materials.

In the case of GaN, nanoparticles are again wrapped in a carbon matrix and partially agglomerated (data not shown). Agglomeration is not surprising and was also observed in a previous contribution.[15] Here, the nanoparticle dispersion could be improved by adjusting the reaction time. HRTEM shown well-developed lattice fringes, with d = 2.43 Å as interplanar distance, corresponding to the plane 101 of the hexagonal structures of gallium nitride (d_{calcd} = 2.43765 Å, ref ICDD-PDF4+ 01−089−7522).

The possibility to switch from nitrides to carbides, say Mo_2N to Mo_2C and W_2N to WC, respectively, simply by changing R was shown in previous work.[9] In spite of the previous observations, it is interesting to search for this effect in the present data set. Changing ratio to very high values seems to affect Nb-, Ti-, and Ga-urea derived samples too, while no remarkably differences in terms on the corresponding XRD patterns have been detected for Cr- and V-samples. We attribute this to their very high nitrophilicity, as already indicated by the release of carbon layers at lower R. For chromium samples, the formation of the corresponding carbide or nitro-carbide at higher R can be strictly excluded, whereas for vanadium samples, the discrimination among nitride, carbide, and intermediate compounds cannot be done unambiguously because of the similarity of the expected XRD patterns.

As a general finding, increasing the R values brings a larger amount of carbon in the final products and a decrease in the amount of nitrogen, as ascertained by elemental analysis (Tables 1 and 2). This means that the composition and coordination environment in the glasses determines the further fragmentation schemes and the composition of the amorphous intermediate particles the final particles crystallize from. As described in our previous paper, this can go until the structure switches into the corresponding stable carbide.

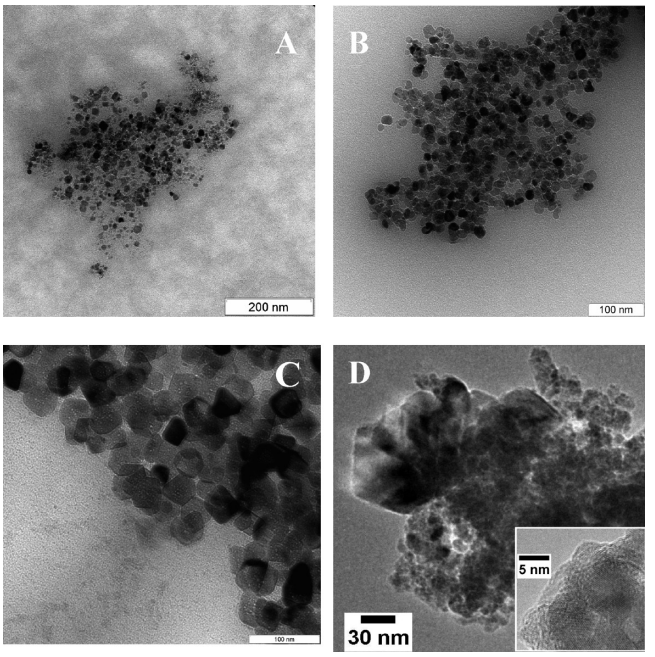

Figure 5. TEM images of urea-derived samples of (A) niobium (R = 12), (B) titanium (R = 10), (C) vanadium (R = 8), and (D) gallium (R = 1).

With the change in elemental composition with R comes changes in both peak positions and peak intensity in the corresponding XRD patterns of the Ti, Nb, and Ga sample (the less nitrophilic species) were observed (Figure 4). Here, one obviously receives not the pure nitrides but the typical textures of heavy heterosubstitution of the structure by carbon on nitride sites. In the same way, XRD pattern of samples prepared at higher R cannot be conclusively attributed to the pure metal carbides, but also here peak shifts and peak intensity variations are found. This makes us believe that especially in case of Ti and Nb samples prepared with higher R and urea (R > 7), a N-doped metal carbide is formed, where carbon is substituted by nitrogen in its unit cell positions. For gallium samples, formation of a ternary or doped compound also cannot be excluded but is less easily revealed from the XRD data.

Experimental and expected lattice parameters for some MN/MC structures are reported in Table SI3 in the Supporting Information.

To support this interpretation, it is important to mention that no traces of structurally diverse side products can be found both by TEM and SEM (Figures 5 and 6,

(15) Buha, J.; Djerdj, I.; Antonietti, M.; Niederberger, M. *Chem. Mater.* **2007**, *19*(14), 3499.

respectively). In particular, SEM allows judging the homogeneity of the samples on the larger scale, which is about perfect in most cases.

The clarification of this matter (amount and type of heterosubstitution, type of defects, etc.), however, relies on more complicated measurements on large-scale instrumentations (such as ESCA, XPS, etc.) and will therefore be the subject of an independent contribution.

For titanium and vanadium nitride, the ratio R affects the size of the synthesized nanoparticles: with increasing R, the diameter increases from 5 to 9 and from 10 to 20 nm, respectively (Tables 1 and 2). We attribute this to the influence of the metal concentration on the nucleation rate in the high-temperature amorphous intermediates.

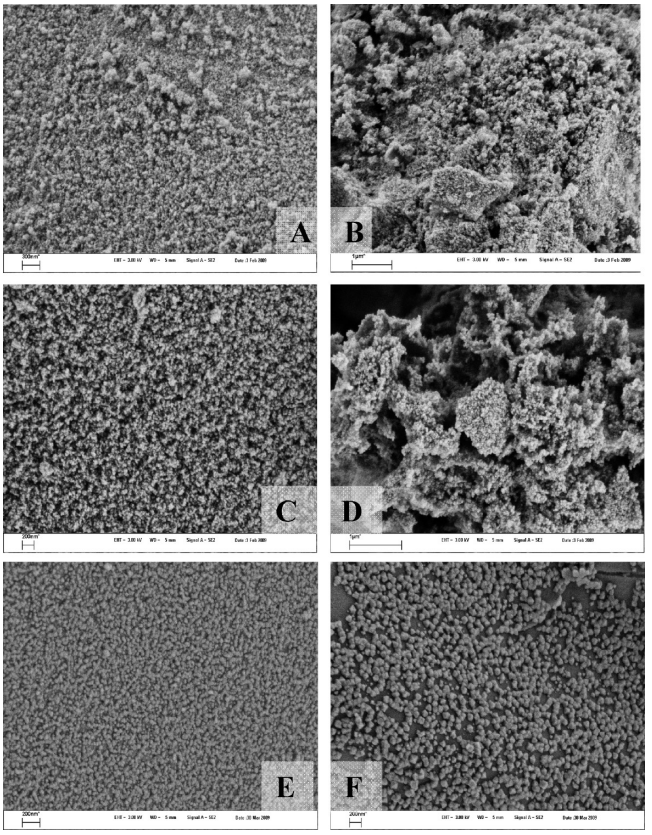

Figure 6. Comparison of SEM images for samples prepared at different urea/metal precursor molar ratios. (A, B) Titanium- ($R = 4$ and $R = 10$, scale bar 300 nm and 1 μm respectively); (C, D) niobium ($R = 3$ and $R = 12$, scale bar 200 nm and 1 μm respectively) and (E, F) vanadium ($R = 3$ and $R = 8$, scale bar 200 nm and 200 nm respectively).

To reveal further mechanistic details of the nanoparticle formation, were performed temperature-dependent measurements. In Figure 7, XRD patterns of titanium and vanadium urea-derived samples treated at different temperature are shown. These are to be regarded as model cases for the two types of behavior found in a broader set of experiments.

The titanium pattern is typical for samples that form the nitrides via a low temperature, easily crystallizing oxide, which here can be easily attributed to TiO_2 as a mixture of anatase and rutile (ref ICDD-PDF4+ 04−007−0701 and 04−008−7848, respectively). This crystalline oxide is then later nitrified by decomposition of the urea and consecutive condensation products. For most other samples, such as vanadium, no crystalline intermediate is formed, and the products obtained at lower temperature ($T < 400$ °C) show the structure of a mixed glass. Heating both types of samples to higher temperatures leads to the formation of the crystalline nitrides. From Figure 7, it is easily seen than further increase of temperature then leads to particle growth, where the diameter increases from ~5 to 9 nm and from ~3 to 25 nm in the case of titanium and vanadium samples, respectively.

To reveal further details of the reaction scheme, TGA measurements were performed on starting titanium and vanadium gels with different compositions and then heated under nitrogen between 50 and 1000 °C (figure 8). The results showed that the conversion progresses in both cases in a few distinct steps. For vanadium, the reaction scheme apparently did not depend on composition. Solvents and precursor fragments are lost until 350 °C until a rather stable mixed glass is formed. Interestingly, this glass converts up to 600 °C under mass loss to the final crystalline structure, which means that the glass most presumably contains an excess of O, N, and C. In the case of titanium, the fragmentation patterns depend on the urea/metal precursor ratio, which is related to the ease of formation of crystalline TiO_2 at lower urea contents. As expected, at higher urea contents, the reaction scheme is much closer to the vanadium case. As already indicated in the previous discussion, this makes

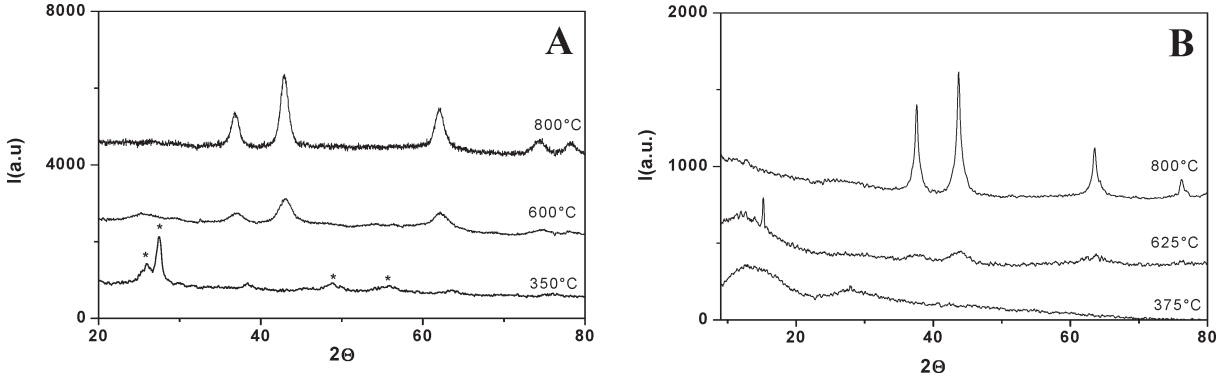

Figure 7. XRD pattern of (A) titanium-urea ($R = 10$) and (B) vanadium-urea ($R = 8$) derived samples treated at different temperature. In (A) marked peaks are attributed to TiO_2.

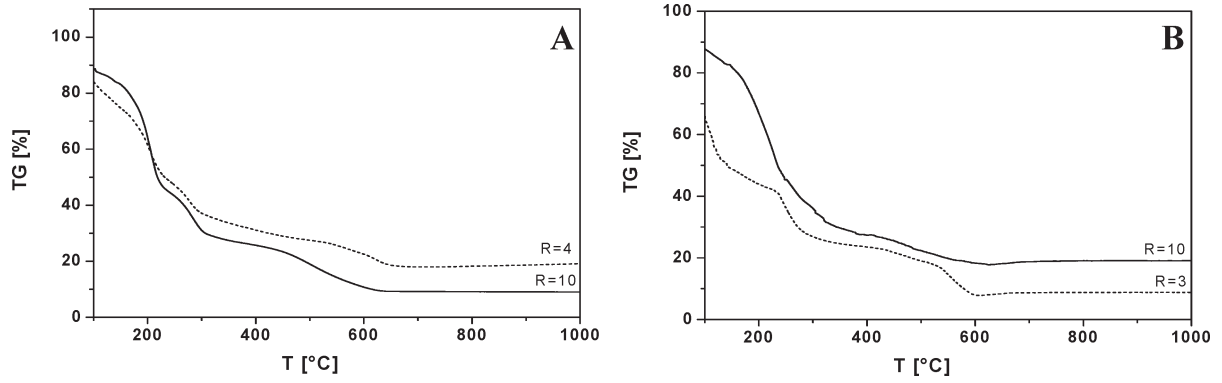

Figure 8. TGA measurements of as prepared (A) titanium and (B) vanadium-urea gels at two different urea/metal precursor's molar ratios (R4 and R3, dotted line; R10, continuous line).

Table 3. Elemental Analysis Results of Some of the 350 °C Glasses

metal precursors	urea/metal precursors molar ratio	N%	C%
$TiCl_4$	4	23.4	12.2
$TiCl_4$	10	33.9	18.2
$VOCl_3$	3	15	9.75
$VOCl_3$	8	22	14.4
$NbCl_5$	3	17.0	7.6
$NbCl_5$	10	29.4	14.9

the structure and composition of the high-temperature amorphous intermediates (above 400 °C) the structure determining key factor.

Elemental analysis performed on the glass intermediate phase at 350 °C confirms an excess of N and C in this phase.

In the case of titanium samples, it contains, indeed, increasing temperature leads to a drastic reduction of C contents (plausibly released in form of corresponding oxides), in line with TiN formation. For higher ratio, increasing temperature also leads to the removal of nitrogen excess from the glass phase, while the carbon amount can be considered unchanged. This finding indirectly confirms the chemical bonding among Ti and C, in line with TiC(N) formation. It worth repeating here that no traces of side products (such as amorphous C) have been observed both by XRD and TEM/SEM investigations.

As expected, behavior of niobium samples was found to be similar to the titanium case. In fact, for lower ratios, the excess of N and C present in the glass phase are lost at $T > 400$ °C, whereas for higher ratios, the drastic reduction of the nitrogen amount with respect to the loss of carbon is in line with a NbC(N) formation.

In the case of vanadium, at lower ratios, the amount of nitrogen and carbon content remains constant increasing the temperature. In line with a glass intermediate where both carbon and nitrogen are bonded to vanadium, at lower temperature, the amount of N and C are comparable and a further increase in temperature does not lead to C reduction but rather an expulsion of the carbon excess, which forms (accordingly with the TEM findings) a coating shell around the particles.

At higher ratios, the intermediate glass phase contains high amounts of carbon and nitrogen, and with increasing temperature, a substitution of C over N (which is successively released in the form of NOx species) seems to occur.

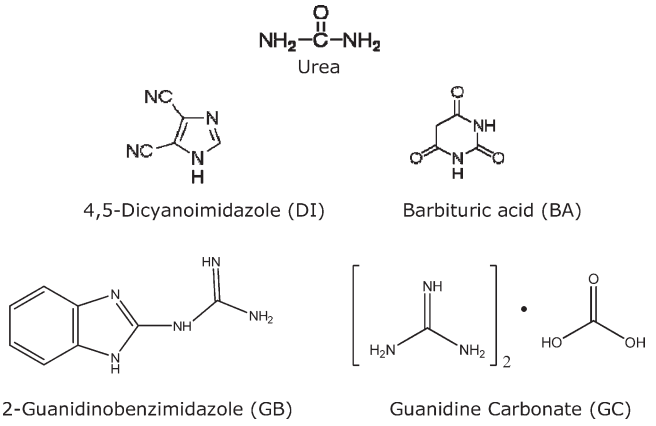

Figure 9. Examples of C/N sources for MC/MN production.

Complementary Carbon/Nitrogen Sources. Up to now it was shown that urea not only allows us to establish a homogeneous starting situation ("the metal-urea-glass") but also provides throughout the decomposition cascade appropriate reducing agents and nitrogen and carbon in a highly dispersed form that can be conveniently alloyed with the metal to form the resulting crystalline nitride or carbide nanostructure. From the perspective of synthetic chemistry, it is interesting to ask if this approach can be extended substituting urea with opportune "similar", easily available starting products, such as barbituric acid (BA), guanidine carbonate (GC), 2-guanidinbenzoimidazole (GB), and 4,5-dicyanoimidazole (DI) (Figure 9). As delineated in the discussion above, one might expect different coordination environments and different glass structures and thereby additional tools for size and composition control.

From this study, it can be said that most of the precursors work rather similar to the urea case, also generating nanosized nitride particles where the trends follow the general observations already made with urea in more detail.

Among the selected precursors, guanidine carbonate and 4,5-dicyanoimidazole were found to have the best behavior for MN/MC production; in particular, we consider the latter as the best candidate to replace urea, plausibly because of the presence of two easily available CN- groups. Indeed, for chromium and niobium samples,

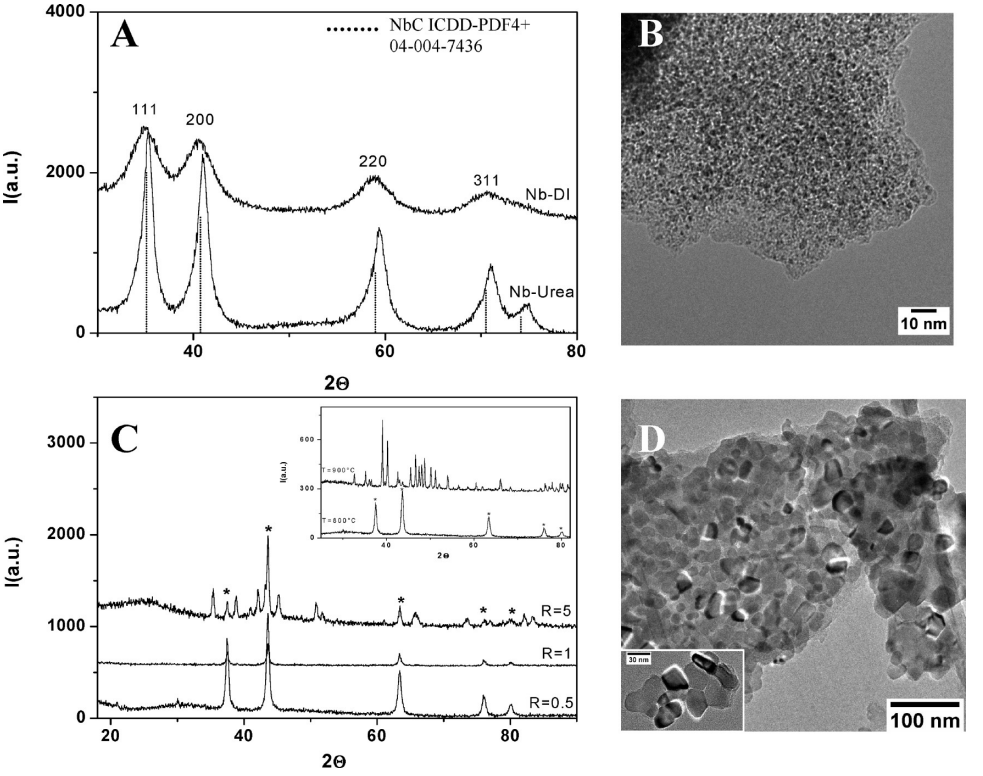

Figure 10. (A) XRD pattern of Nb samples prepared using urea ($R = 10$) and DI ($R = 5$) as C source, respectively (calculated pattern of NbC is also reported as dotted lines), and (B) TEM image of Nb-DI derived sample ($R = 5$). (C) XRD patterns of Cr-DI derived samples prepared with different DI/metal precursor molar ratio and treated at 800 °C. In the inset a comparison between Cr-DI samples ($R = 0.5$) treated at two different temperatures. Marked peaks are attributed to CrN and not market to Cr_3C_2. (D) TEM image of Cr-DI derived sample ($R = 0.5$), treated at 800 °C.

the use of 4,5-dicyanoimidazole allows the direct synthesis of Cr_3C_2 and NbC respectively, which was not possible with urea (Figure 10).

The procedure is similar to the urea pathway: appropriate amounts of ethanol (usually 2 g) were mixed with an adequate amount of the selected metal precursor (0.5−1 g) to reach a target concentration. A varying amount of solid C/N source was then added slowly to the alcoholic solution to give the specific urea/metal precursor molar ratio (R), stirring until the solution was completely clear (experimental details are reported in Table SI2 in the Supporting Information).

The gels were then put into an oven and treated under N_2 flow at the selected temperature for 3 h (plus 4 h to reach the final temperature). Also in this case, a dark finely dispersed powder has been obtained, and no further purification has been done before or after the temperature treatment.

In the case of niobium, very small, strongly interacting nanoparticles (typical for unprotected particles) are found. Although the primary particle size is around 2.5 nm (as estimated by XRD), only rather dense and smooth aggregates are observed, with no single particle being separated (Figure 10A, B). Similar results have been found using guanidine carbonate (data not shown).

In the case of chromium, switching from nitride to carbide is possible simply by changing the DI/metal precursor molar ratio (figure 10.C) or heating temperature (Figure 10C, inset). At lower ratio and $T = 800$ °C pure CrN was obtained. TEM investigation on this sample showed, together with smaller (primitive) particles ($d < 10$ nm), larger close-packed crystals ($d \approx 30$ nm) with metallic behavior (Figure 10D). Detailed experiments are here in progress but preliminary studies shown that more defined structures can be obtained increasing the reaction time (Figure SI2B in the Supporting Information).

Interesting for understanding the reaction mechanism, chromium samples prepared at $T \leq 800$ °C result in Cr_3C_2 at $R > 5$ (ref ICDD-PDF4+ 03−065−0897, space group *Cmcm*-63) but are still accompanied by CrN generation (ref ICDD-PDF4 + 04−008−7177) and traces of amorphous carbon (large peak around 26°). For $T \geq 900$ °C, pure Cr_3C_2 can be obtained already at $R = 0.5$ but, surprisingly, different space group (ref ICDD-PDF4 + 04−007−1407, space group *Pnma*-62) and higher amounst of carbon as side product.

Preliminary experiments performed using the two guanidine derivates shown different behavior. The low solubility of chromium chloride in guanidine carbonate did not allow proceeding further while the higher solubility in 2-guanidinobenzoimidazole allowed us to investigated different ratios ($R_{max} = 3$), but in each case, a mixture of chromium nitride and carbide has been found (although different in composition as MN predominates at lower R while MC predominates at higher R).

In the case of vanadium and titanium samples, the major restriction lies in the lower solubility of these sources in alcohols. Both guanidine-carbonate and barbituric acid have been tested, and in both cases $R > 1$ was

never reached. It is not surprising that the then synthesis partially fails, bringing mixtures of nitride and oxide (data not shown).

This variation of the nitrification/carbidization reagents also allows us to summarize all data to an at least cohesive reaction mechanism. In this view, the "urea glass route" is to be seen as a combination/chimera between sol−gel chemistry and a carbothermal reduction nitridation process (CRN).[16,17] First, by dissolution of the chlorides in alcohol and subsequent removal of HCl and excess alcohol/water, we create metal orthoesters that condense to a gel where the secondary ligation of the metal with urea sets a coordination environment all further reactions are controlled from. The metal centers in this state are most presumably still linked via oxygen functionalities, as covalent M−N and M−C bonds are hard to form at those low temperatures.

TGA indicates that this gel further condenses to a "urea glass" or glassy amorphous intermediates, the formation of which is completed at around 400 °C. By choice of the organic precursor and the relative stoichiometry, we can control the composition of this glass, which for sure contains, beside the metal ions, oxygen, carbon, and nitrogen.

Further increase of temperature results in further condensation of this disordered mixture under mass loss and practical (in most cases) complete removal of the oxygen, then to crystallization of the diverse nanoparticles from this environment. It is important for the understanding of the process that the metal centers usually seriously change the oxidation state at this point, which is usually−beyond formal Coulombic charge equivalents−a reduction. Loss of oxygen and reduction of the metal centers is usually called carbothermal reduction (e.g., the manufacturing of iron) but here more appropriately described as a carbothermal reduction nitridation process (CRN). This process is mass wise completed at around 600 °C, but development of the perfected crystalline structure of the final product might take up to temperatures of 900 °C, which is regarded to be classical recrystallization from more disordered states and smaller nanoparticles. In this phase, recrystallization of the more nitridophilic can obviously also create very well-defined, thin carbon shells around the nanostructures, which−as in zone melting−can be regarded as the product of the out-diffusion of carbon species from the precursor states

In this sort of carbothermal reduction nitridation, nitrogen and carbon compete in bonding metal atoms, leading to MN or MC or cross-wise doped compounds, while the formation of mixture MN+MC has been hardly observed. The reaction outcome can thereby piloted−mostly between all three possible species, simply by playing with some factors such as concentration and nature of C/N source and/or nature of the metal precursors, as well as temperature and reaction time. The key point for the generation of nanoparticles is the close contact of the C source with the reduced species, which is more difficult to obtain when mixing crystalline (solid) phases or by gas−solid phase reactions then in a gel phase. Here, the interface among the reacting species is increased and the gaseous diffusion of the reductive species improved. This is probably the reason why this procedure can lead to metal carbides and metal nitrides at comparably moderate temperatures with high definition and structural control.

(16) Eick, B. M.; Youngblood, J. P. *J. Mater. Sci.* **2009**, *44*(5), 1159.
(17) Vaidhyanathan, B.; Rao, K. J. *Chem. Mater.* **1997**, *9*(5), 1196.

Conclusions

In the present article, we generalize a previously described procedure suitable as starting point for preparing nanostructured, tailored metal nitrides and metal carbides and their ternary compounds. Simply by adjusting intensive variables as concentration and temperature, the demanded product can be obtained in a rather simple, relatively cheap and fast way. No preliminary treatments or further purification steps of the products are in fact needed. The high versatility of this new route as well as its general usefulness to produce very fine particles with high specific surface area has been shown for a broader set of metal salts.

Furthermore, more complex and refined structures, such as CrN@C nanocomposites and mesoporous VN structures, were found. Finally, by the "glass route", it is possible in many cases to switch from MN to MC simply by changing the composition of the intermediary glass phases. It has also been shown that procedure can be further broadened by exchanging urea by related compounds, and a different reactivity of the metal precursors toward the different C/N sources has been observed. In particular, 4,5-dicyanoimidazole can be recommended as a complementary C/N source, supporting the formation of some critical nanometal carbides, such as Cr_3C_2 and NbC.

We believe that by avoiding the metal oxide formation step, this procedure could broaden the access to MN or MC materials in general, e.g., for compounds where the corresponding metal oxide is difficult to prepare, or not easy to nitrify/carburize, while probably simultaneously decreasing the necessary reaction time and temperature.

A peculiar and special advantage of this new route is in principle liquid/jelly/glassy starting materials that allow recombination with top down processes, i.e., the application of microstructured reaction zones by dipping, coating, ink jet printing, or replication techniques. This might significantly simplify integration of MN and MC nanostructures into more complex devices and chemical systems.

Acknowledgment. The authors are grateful to the Fritz Haber Institute of the Max Planck Society/Berlin for HR-TEM measurements and to Ms. Katharina Ostwald for the precious help in our laboratory. We also thank the BASF Company and the Max Planck Society for the financial support.

Supporting Information Available: Additional figures and tables (PDF). This material is available free of charge via the Internet at http://pubs.acs.org.